






Presenilin Is Essential for ApoE Secretion, a Novel Role of Presenilin Involved in Alzheimer's Disease Pathogenesis

Sadequl Islam,¹ Yang Sun,¹ Yuan Gao,¹  Tomohisa Nakamura,¹ Arshad Ali Noorani,¹ Tong Li,²  Philip C. Wong,² Noriyuki Kimura,³ Etsuro Matsubara,³ Kensaku Kasuga,⁴  Takeshi Ikeuchi,⁴  Taisuke Tomita,⁵  Kun Zou,¹ and Makoto Michikawa¹

¹Department of Biochemistry, Graduate School of Medical Sciences, Nagoya City University, Nagoya 467-8601, Japan, ²The Solomon H. Snyder Department of Neuroscience, Johns Hopkins University School of Medicine, Baltimore, Maryland 21205, ³Department of Neurology, Faculty of Medicine, Oita University, Oita 870-1192, Japan, ⁴Department of Molecular Genetics, Brain Research Institute, Niigata University, Niigata 951-8585, Japan, and ⁵Laboratory of Neuropathology and Neuroscience, Faculty of Pharmaceutical Sciences, University of Tokyo, Tokyo 113-0033, Japan

Alzheimer's disease (AD) is a debilitating dementia characterized by progressive memory loss and aggregation of amyloid- β ($A\beta$) protein into amyloid plaques in patient brains. Mutations in presenilin (PS) lead to abnormal generation of $A\beta$, which is the major cause of familial AD (FAD), and apolipoprotein E4 (ApoE4) is the major genetic risk factor for sporadic AD (SAD) onset. However, whether dysfunction of PS is involved in the pathogenesis of SAD is largely unknown. We found that ApoE secretion was completely abolished in PS-deficient cells and markedly decreased by inhibition of γ -secretase activity. Blockade of γ -secretase activity by a γ -secretase inhibitor, DAPT, decreased ApoE secretion, suggesting an important role of γ -secretase activity in ApoE secretion. Reduced ApoE secretion is also observed in nicastrin-deficient cells with reduced γ -secretase activity. PS deficiency enhanced nuclear translocation of ApoE and binding of ApoE to importin α 4, a nuclear transport receptor. Moreover, the expression of PS mutants in PS-deficient cells suppressed the restoration effects on ApoE secretion compared with the expression of wild-type PS. Plasma ApoE levels were lower in FAD patients carrying PS1 mutations compared with normal control subjects. Our findings suggest a novel role of PS contributing to the pathogenesis of SAD by regulating ApoE secretion.

Key words: apolipoprotein E; familial AD; presenilin; secretion; sporadic AD

Significance Statement

Familial AD (FAD) typically results from mutations in the genes encoding amyloid precursor protein, presenilin 1 (PS1), or PS2. Many PS mutants have been found to exert impaired γ -secretase activity and increased amyloid- β 42 ($A\beta$ 42)/ $A\beta$ 40 ratio, which induce early amyloid deposition and FAD. On the other hand, apolipoprotein E4 (ApoE4) is the major genetic risk factor for sporadic AD (SAD) and contributes to AD pathogenesis because it has reduced $A\beta$ clearance capability compared with ApoE3 and ApoE2. FAD and SAD have long been considered to be caused by these two independent mechanisms; however, for the first time, we demonstrated that PS is essential for ApoE secretion and PS mutants affected ApoE secretion *in vitro* and in human samples, suggesting a novel mechanism by which PS is also involved in SAD pathogenesis.

Received Oct. 10, 2021; revised Dec. 13, 2021; accepted Dec. 19, 2021.

Author contributions: K.Z. and M.M. designed research; S.I., Y.S., Y.G., T.N., A.A.N., T.L., P.C.W., N.K., E.M., K.K., T.I., T.T., and K.Z. performed research; S.I. and K.Z. analyzed data; S.I. and K.Z. wrote the paper.

This work was supported by the Grant-in-Aid for Scientific Research B 16H05559 (to M.M.), Challenging Exploratory Research Grant 15K15712 (to M.M.), and Grant-in-Aid for Scientific Research C 19K07846 (to K.Z.) from the Ministry of Education, Culture, Sports, Science, and Technology, Japan. This work was also supported by "Project of Translational and Clinical Research Seed A" Grant A-128 (to M.M.); "Research and Development Grants for Dementia" Grants AMED 21dk0207050h0002 (to M.M.), AMED JP21dk0207049, and JP21dk0207045 (to T.I.); and Grants-in-aid from "The 24th General Assembly of the Japanese Association of Medical Sciences" (to K.Z.), the Daiko Foundation (to K.Z.), and the Hirose International Scholarship Foundation (to K.Z.). S.I. was supported by the Ministry of Education, Culture, Sports, Science, and Technology, Japan. We thank Dr. Bart De Strooper for providing wild-type, PS double knock-out (PS1/2^{-/-}), PS1 knock-out (PS1^{-/-}), and PS2 knock-out (PS2^{-/-}) mouse embryonic fibroblast cells.

The authors declare no competing financial interests.

Correspondence should be addressed to Kun Zou at kunzou@med.nagoya-cu.ac.jp or Makoto Michikawa at michi@med.nagoya-cu.ac.jp.

<https://doi.org/10.1523/JNEUROSCI.2039-21.2021>

Copyright © 2022 the authors

Introduction

Alzheimer's disease (AD) is the most common form of dementia, and its pathologic hallmarks include the deposition of extracellular amyloid- β ($A\beta$) protein aggregates as amyloid plaques in patient brain (Scheltens et al., 2016). The intramembrane protease γ -secretase proteolytically process amyloid precursor protein (APP), to generate a series of amyloidogenic $A\beta$ with 39–43 aa in the brains of AD patients (Golde et al., 1992; De Strooper et al., 2012). The mature γ -secretase protease consists of four components: presenilin (PS), nicastrin (NCT), anterior pharynx-defective 1 (APH-1), and PS enhancer 2 (PEN-2; Kimberly et al., 2003; Bai et al., 2015). Clinically, AD is divided into sporadic AD (SAD) and familial AD (FAD). FAD cases are caused by dominantly inherited genetic mutations in an individual carrying a

mutation that confers disease in an autosomal-dominant inheritance pattern. While it is hypothesized that SAD arises because of reduced clearance of $A\beta$, this has not been definitively proved (Kanekiyo et al., 2014). Reliable estimates of the prevalence of FAD are 1–5%, and the prevalence of SAD accounts for >95% of all AD cases (Scheltens et al., 2016). FAD was found to be genetically linked to missense mutations either in PS or APP, and consistently increase the relative ratio between the long ($A\beta$ 42) and short ($A\beta$ 40) amyloid peptides (Scheuner et al., 1996; Huang and Mucke, 2012). Most mutations in the PS1 and PS2 genes lead to elevated molar ratios of $A\beta$ 42/ $A\beta$ 40 (Borchelt et al., 1996; Sun et al., 2017), which is responsible for the early onset of FAD (Scheuner et al., 1996; Huang and Mucke, 2012; Watanabe and Shen, 2017).

Polymorphism in the apolipoprotein E (ApoE) gene is a major genetic risk determinant of SAD, with the ApoE4 allele conferring a stronger genetic risk factor for AD than the more common ApoE3 allele, whereas the presence of the ApoE2 allele conferring a decreased risk for AD (Strittmatter et al., 1993; Yamazaki et al., 2019). ApoE is one of the major apolipoproteins that regulate lipid and cholesterol transport and delivery through cell surface ApoE receptors (Mahley, 1988; Michikawa et al., 2000; Kanekiyo et al., 2014). Mounting evidence suggests that the ApoE4 protein isoform drives amyloid pathology through the disturbance of $A\beta$ clearance machinery, leading to $A\beta$ accumulation in the brain and an increased risk for the pathogenesis of AD (Liu et al., 2013). Much evidence from *in vivo* studies has shown that $A\beta$ clearance is slower in ApoE4-TR mice compared with ApoE3-TR mice (Castellano et al., 2011). Indisputable evidence demonstrated that ApoE4 knock-in (KI) mice have greater $A\beta$ deposition compared with ApoE3 knock-in mice (Holtzman et al., 2000; Li, 2019); whereas human ApoE2-expressing mice showed the dramatic reduction of $A\beta$ deposition (Fagan et al., 2002; Li, 2019). These findings suggest that clearance of $A\beta$ by ApoE is important for preventing $A\beta$ deposition for AD onset and that the regulation of ApoE metabolism by other molecules can affect $A\beta$ clearance.

Together, PS and ApoE have crucial and diverse roles, respectively, in FAD and SAD pathogenesis. Analysis of 138 distinct FAD-derived PS1 mutations revealed that 90% of the analyzed mutations impaired γ -secretase-dependent cleavage of APP, as shown by reduced production of $A\beta$ 40 and increased $A\beta$ 42/ $A\beta$ 40 ratio. However, some of the PS mutations lead to reduced $A\beta$ 42/ $A\beta$ 40 ratio (Sun et al., 2017). These findings suggest that PS may be involved in AD pathogenesis by different mechanisms other than regulating $A\beta$ generation. PS is a multifunctional molecule and has several functions in addition to serving as γ -secretase. The γ -secretase-independent functions of PSs include stabilizing β -catenin in Wnt signaling pathway; regulating calcium homeostasis; and regulating autophagy, protein trafficking, and apoptosis, and their interaction with synaptic transmission (De Strooper et al., 2012; Zhang et al., 2013; Duggan and McCarthy, 2016). We hypothesized that PS or PS functions may be involved in ApoE metabolism or secretion. Herein, we found a novel role of PS in regulating ApoE secretion: that is, PS is essential for ApoE secretion and PS mutations exert impaired ApoE secretion *in vitro* and *in vivo*. For the first time, our findings suggest a novel mechanism by which PS is also involved in AD pathogenesis via regulating ApoE secretion.

Materials and Methods

Cell culture. Wild-type (WT), PS double-knock-out (PS1/2^{-/-}), PS1 knock-out (PS1^{-/-}), and PS2 knock-out (PS2^{-/-}) mouse embryonic

fibroblast (MEF) cells were provided by Bart De Strooper, Department of Neurosciences, Leuven Brain Institute, Leuven 3000, Belgium (Herreman et al., 1999). NCT knock-out (NCT^{-/-}) MEF cells were previously generated from NCT-deficient mouse embryos (Li et al., 2003a). Cell lines were maintained in DMEM (Thermo Fisher Scientific) containing 10% fetal bovine serum (FBS). WT, PS1/2^{-/-}, PS1^{-/-}, PS2^{-/-}, and NCT^{-/-} cells were cultured for 48 h in serum-free DMEM to analyze ApoE secretion. A total of 14 ml of serum-free DMEM culture supernatant was centrifuged at 5000 × *g* at 4°C using a centrifugal filter unit (Amicon Ultra-15; catalog #UFC901024, Millipore) to a final volume of 200 μ l. The amount of sample used for the examination of secreted ApoE levels was normalized based on the total protein level and was subjected to SDS-PAGE and Western blotting.

Highly astrocyte-rich cultures were prepared according to a method described previously (Isobe et al., 1999). In brief, the brain was removed from 18-d-old WT C57BL/6J mouse embryos under anesthesia. The cerebral cortex was dissected, freed from the meninges, and minced into small pieces. The cortical fragments were incubated in 0.25% trypsin and 20 mg/ml DNase I in PBS (8.1 mM Na₂HPO₄, 1.5 mM KH₂PO₄, 137 mM NaCl, and 2.7 mM KCl, pH 7.4) at 37°C for 20 min. The fragments were then dissociated into single cells by repeated pipetting. The dissociated cells were seeded in 75 cm² dishes at a density of 1 × 10⁷ cells in DMEM containing 10% FBS. After 7 d of incubation *in vitro*, astrocytes in the monolayer were trypsinized (0.1%) and reseeded. The astrocyte-rich cultures were maintained in DMEM containing 10% FBS until use. Primary cultured MEFs were prepared according to a method described previously, with some modifications (Li et al., 2003a). Briefly, skin from 18-d-old embryos of WT C57BL/6J mice or postnatal day 1 ApoE3-KI C57BL/6NcrSlc mice was minced, suspended in 0.25% trypsin and 20 mg/ml DNase I in PBS, incubated at 37°C for 20 min, and then seeded in 75 cm² flasks. The cultures were maintained in DMEM containing penicillin and streptomycin (50 μ g/ml) and 10% FBS until use.

Western blotting. Cultured cells were rinsed twice with ice-cold PBS and homogenized in lysis buffer (25 mM Tris-HCl, pH 7.6, 150 mM NaCl, 1% Nonidet P-40, 1% sodium deoxycholate, 0.1% SDS) containing a protease inhibitor cocktail (Roche) for 30 min at 4°C, then centrifuged at 14,000 rpm for 5 min at 4°C. Equal amounts of protein from the cell lysate were dissolved in 4× SDS sample buffer (250 mM Tris-HCl, pH 6.8, 40% glycerol, 8% SDS, and 0.01% bromophenol blue) and heated for 5 min at 95°C for denaturation. Proteins were separated by SDS-PAGE and blotted onto polyvinylidene difluoride membranes (Sigma-Aldrich). The membranes were then probed overnight with specific primary antibodies at 4°C. Appropriate peroxidase-conjugated secondary antibodies were applied, and the blots were visualized using Super Signal Chemiluminescence solution (Wako) according to the manufacturer instructions. Membranes were then stripped and reprobed with anti- α -tubulin antibody. Quantification was performed using ImageJ software (National Institutes of Health). Detailed information regarding antibodies is provided in Table 1. Antibody validation profiles are available on the websites of the companies from which the antibodies were sourced.

Immunostaining. Cells were seeded and incubated at 37°C for 24 h, then fixed in cold 4% paraformaldehyde for 30 min at room temperature. The cells were then permeabilized with 0.1% Triton X-100 and blocked for 60 min in 10% normal donkey serum in Tris-buffered saline (TBS) with Tween 20 cells were then incubated with the proper primary antibodies for 12 h at 4°C. Immunostaining for ApoE and importin α 4 colocalization in WT and PS1/2^{-/-} cells was accomplished using anti-ApoE (F-9) and anti-importin α 4 primary antibodies. Immunofluorescent labeling was accomplished using Alexa Fluor 488-tagged or Alexa Fluor 568-tagged secondary antibodies (Thermo Fisher Scientific). Before mounting onto slides, cells were stained with 4',6'-diamidino-2-phenylindole dihydrochloride (DAPI; Prolong Gold Antifade Reagent, Thermo Fisher Scientific) and subjected to confocal microscopy. Images were captured using an Olympus FV 3000 confocal microscope (with an oil-immersion plan Apo 60× A/1.40 numerical aperture objective lens. Detailed information regarding antibodies is provided in Table 1.

Confocal imaging and analyses. Confocal images were acquired as described in the previous section. Laser and detector settings were

Table 1. Information regarding antibodies, reagents, and assay kits

Reagent or resource	Source	Identifier
Primary antibodies		
Anti-ApoE	EMD Millipore	Catalog #AB947
Anti-ApoE (F-9)	Santa Cruz Biotechnology	Catalog #sc-390925
Anti-PS1 CTF	Merck Millipore	Catalog #MAB5232
Anti-PS2 CTF	Abcam	Catalog #ab51249
Anti-PEN2	Abcam	Catalog #ab18189
Anti-APH-1a CTF	BioLegend	Catalog #PRB-550P
Anti-NCT	Sigma-Aldrich	Catalog #N1660
Anti-cleaved Notch1 (Val1744)	Cell Signaling Technology	Catalog #4147
Anti-KPNA4/IPOA3/importin α 3	Everest Biotech	Catalog #EB06238
Anti-KPNA3/IPOA4/importin α 4	Everest Biotech	Catalog #EB06237
Anti-PARP	Sigma-Aldrich	Catalog #P7605
Anti- α -tubulin	Sigma-Aldrich	Catalog #T9026
Secondary antibodies		
Anti-Mouse IgG HRP-linked antibody	Cell Signaling Technology	Catalog # 05/2019
Anti-rabbit IgG HRP-linked antibody	Cell Signaling Technology	Catalog # 09/2019
Anti-Goat IgG HRP-linked antibody	Merck Millipore	Catalog #AP186P
Secondary antibodies for immunofluorescence staining		
Alexa Fluor 488 donkey anti-mouse IgG (H + L)	Thermo Fisher Scientific	Catalog #A-21202
Alexa Fluor 488 donkey anti-rabbit IgG (H + L)	Thermo Fisher Scientific	Catalog #A-21206
Alexa Fluor 568 donkey anti-goat IgG (H + L)	Thermo Fisher Scientific	Catalog #A-11057
Chemicals and antibiotics		
DAPT	Tocris Bioscience	Catalog #2634
Polybrene	Santa Cruz Biotechnology	Catalog #sc-134220
Puromycin dihydrochloride	Santa Cruz Biotechnology	Catalog #sc-108071
FuGENE HD transfection reagent	Promega	Catalog #E231A
Penicillin-streptomycin solution ($\times 100$)	Wako	Catalog #168–23191
DAPI	Thermo Fisher Scientific	Catalog #P36931
Critical commercial assays		
ELISA human/rat A β 40	Wako	Catalog #294–64701
ELISA human/rat A β 42	Wako	Catalog #290–62601
ELISA human/rat A β 42, high sensitive	Wako	Catalog #292–64501
Human ApoE (AD2) ELISA Kit	Thermo Fisher Scientific	Catalog #EHAPOE

maintained properly for the acquisition of each target molecule. For all analyses, images were acquired from different cells and slides using a $60\times$ oil differential interference contrast objective at 2048×2048 or 1024×1024 pixel resolution, respectively. For quantification of cytosolic and nuclear ApoE pixel intensity, acquired images were imported to ImageJ software. Nuclear boundaries were determined by staining with 4',6-diamidino-2-phenylindole (DAPI; catalog #P36931, Thermo Fisher Scientific). Mean staining intensity of cytosolic and nuclear ApoE was determined for each region of interest. Colocalization of ApoE with importin α 4 was quantified using ImageJ software. Threshold intensity was determined using the thresholding function and preset for both fluorescent signals. Pixel intensity for colocalized images was quantified and scored automatically when above the threshold intensity, which was expressed as colocalized mean intensity.

Subcellular fractionation. Cell-free cytoplasmic and nuclear extracts were prepared as described previously (Theendakara et al., 2016), with some modifications. Briefly, cells were lysed in ice-cold fractionation buffer (20 mM HEPES, pH 7.4, 10 mM KCl, 250 mM sucrose, 1.5 mM $MgCl_2$, 1 mM EDTA, 1 mM EGTA, 1 mM dithiothreitol, and protease inhibitor mixture) and sonicated briefly, and then the nuclei were pelleted by centrifugation for 10 min at $750\times g$. The supernatant was then centrifuged at $100,000\times g$ for 30 min. The resulting supernatant contained the soluble cytosolic fraction. The pellets were resuspended in ice-cold fractionation buffer and sonicated three times for 30 s each, and then the debris was removed by centrifugation for 10 min at $4^\circ C$ and $20,000\times g$. Equal amounts of protein (120 μg) were subjected to SDS-PAGE and Western blotting analysis. Membranes were probed with anti-ApoE antibody. The purity of the nuclear fraction was assessed by the presence of poly(ADP-ribose) polymerase (PARP).

Blue native PAGE. WT, PS1 $^{2-/-}$, PS1 $^{-/-}$, PS2 $^{-/-}$, and NCT $^{-/-}$ MEFs were lysed in native sample buffer (Thermo Fisher Scientific) containing 1% digitonin and a protease inhibitor mixture. Lysates were then

briefly sonicated and centrifuged at $20,000\times g$ at $4^\circ C$ for 5 min; the supernatant was separated on a 4–16% Bis-Tris gel (Thermo Fisher Scientific) according to the instructions of the Novex Bis-Tris gel system (Thermo Fisher Scientific). The γ -secretase complex was probed using antibodies against PS1-C-terminal fragment (CTF), PS2-CTF, APH-1, and NCT.

Infection of WT PS and PS mutants. For the expression of human WT PS1, WT PS2, or PS mutants (PS1 Δ E9, PS1L166P, PS1G384A, and PS2N141I), cDNAs were inserted into the EcoRI site of pMXs-puro (Kitamura et al., 2003). The retroviral plasmids were transfected into platinum-E cells using FuGENE (catalog #E231A, Promega) for retroviral packaging (Kitamura et al., 2003; Watanabe et al., 2005; Futai et al., 2016). After 24 h, the conditioned medium was collected and used as viral stock. For highly efficient retroviral infection, cells were cultured with viral stock containing 5 $\mu g/ml$ polybrene (catalog #sc-134220, Santa Cruz Biotechnology) and were allowed to proceed for PS expression. To determine the efficacy of retroviral infection of cells, virus stock was added to new medium containing 10% FBS and puromycin (1 $\mu g/ml$) immediately before use. After 24 h, the virus stock was replaced with fresh serum-free medium (lacking virus) and allowed to proceed for PS expression.

Human plasma. Plasma was collected from living FAD patients and normal age-matched control subjects using standard methods (Abdullah et al., 2019). All relevant guidelines and regulations were strictly followed for all methods. For plasma collection, 12 FAD patients carrying PS1 mutations who visited Niigata University Hospital were enrolled. Plasma samples were also obtained from 12 normal control subjects who visited Oita University Hospital. Detailed information about the sex, age, age of AD onset, age of blood taking, and ApoE genotype of these patients is provided in Table 2. The samples were aliquoted after collection and immediately stored at $-80^\circ C$ until use. The average age of the subjects of the normal control group was 55.58 ± 1.96 years, and that of the subjects of the FAD group carrying PS1 mutations was 51.04 ± 2.30 years (data

Table 2. Information of normal controls and FAD patients with various PS1 mutations

NC group				FAD group				
Normal control subject no.	Sex	Age of taking blood (years)	ApoE genotype	FAD patient (PS1 mutation)	Sex	Age of taking blood (years)	Age of AD onset (years)	ApoE genotype
NC-1	F	44	Unknown	M146I	M	41	40	3/3
NC-2	M	47	4 (–)	L418W	F	42.5	34	3/3
NC-3	M	47	4 (–)	M139V	F	45	41	3/4
NC-4	M	52	4 (–)	L420R	F	45	40	2/3
NC-5	M	55	4 (–)	H214P	F	47	46	3/3
NC-6	F	55	4 (–)	E273A	F	47	45	3/3
NC-7	F	57	4 (–)	P264L	F	52	48	3/4
NC-8	M	61	4 (–)	L282F	M	54	54	3/3
NC-9	F	61	Unknown	P88L	F	54	52	3/3
NC-10	F	62	4 (–)	G209A	F	56	48	3/3
NC-11	F	63	Unknown	G217V	F	62	55	3/3
NC-12	F	63	Unknown	E123K	M	67	64	3/3

F, Female; M, male; NC, normal control subject.

represent the mean \pm SEM; $p = 0.1469$, unpaired two-tailed t test). The clinical diagnosis of AD was made according to the criteria of the National Institute of Neurologic and Communicative Diseases and Stroke/Alzheimer's Disease and Related Disorders Association. All subjects underwent clinical examination that included biochemical, molecular biological, and genomic testing. Experiments using human plasma were performed after obtaining informed consent from each subject. ApoE levels in the plasma of FAD patients and normal age-matched control subjects were determined using a human ApoE (AD2) ELISA kit (EHAPOE, Thermo Fisher Scientific). The ethics committees of Oita University Hospital, Niigata University Hospital, and Nagoya City University Hospital approved the study.

Mice. WT C57BL/6J mice were obtained from SLC. All mice were bred on a 12 h light/dark schedule with *ad libitum* access to standard chow (CE-2, CLEA) and tap water. ApoE3-KI C57BL/6NCrSlc mice expressing human ApoE3 instead of mouse ApoE were generated using gene-targeting techniques, taking advantage of homologous recombination in embryonic stem cells (KI), as reported previously (Gong et al., 2002). Postnatal day 1 mice harboring the homozygous E3 (3:3) allele and correctly expressing human ApoE3 protein were used in this study for generating primary fibroblasts. Ten-week-old WT C57BL/6J mice ($n = 12$; 6 male and 6 female) were divided into two groups (each group containing three males and three females) and administered vehicle (DMSO) or DAPT (100 mg/kg) for 48 h via intraperitoneal injection. The dose of DAPT for *in vivo* experiments was determined according to previous studies (Comery et al., 2005). At the end of the study, the mice were killed by intraperitoneal administration of a combination of anesthetics: medetomidine (0.3 mg/kg), midazolam (4 mg/kg), and butorphanol (5 mg/kg). CSF was then collected via the cisterna magna, the opening between the cerebellum and dorsal surface of the medulla oblongata. Mice were then transcardially perfused with cold PBS, and the brain was immediately collected from each mouse and frozen at -80°C until use. The experiments in this study were performed in strict accordance with the recommendations of the Fundamental Guidelines for Proper Conduct of Animal Experiments and Related Activities in Academic Research Institutions, under the jurisdiction of the Ministry of Education, Culture, Sports, Science and Technology, Japan.

ELISA. Levels of A β 40 and A β 42 peptides were measured using a sandwich ELISA according to the manufacturer instructions (Wako Pure Chemical Industries). The cortices of DMSO- and DAPT-treated mice were homogenized in 19 volumes of ice-cold TBS (10 mM Tris-HCl and 150 mM NaCl, pH 7.6) containing a protease inhibitor cocktail (Roche). The resulting homogenates were centrifuged at 100,000 rpm for 20 min at 4°C . The pellets were washed with ice-cold TBS, and then 10 volumes of 5 M guanidine hydrochloride were added to the pellets. The samples were sonicated and incubated at room temperature for 1 h. The homogenates were centrifuged at 100,000 rpm for 20 min at 4°C , and the resulting supernatants were transferred to new tubes and used for A β determination. The amounts of A β 40 and A β 42 were

determined using ELISA kits (Wako Pure Chemical Industries). The brain homogenates were further diluted 1:8 for A β 40 and 1:15 for A β 42 using the dilution buffer provided with the ELISA kit (Wako). Levels of A β 42 were determined using a highly sensitive ELISA because of the low level of A β 42 in WT C57BL/6 mice. A β levels were normalized to brain tissue weight. Fibroblasts stably expressing human APP695 (Zou et al., 2007) were grown in DMEM (Thermo Fisher Scientific) containing 10% FBS. The medium was changed when the cells reached 100% confluence, and the fibroblasts were treated with DAPT or with DMSO as a vehicle control. The levels of A β 40 and A β 42 in the medium were determined 48 h after treatment of fibroblasts with DAPT. All samples were analyzed in quadruplicate.

The sandwich ELISA for ApoE was performed according to the instruction manual of the Human ApoE (AD2) ELISA kit (EHAPOE, Thermo Fisher Scientific). Briefly, all reagents and samples were brought to room temperature (18 – 25°C) before use. Human plasma samples were diluted 1000-fold using $1\times$ assay diluent. A total of 100 μl of standard or sample was added to appropriate wells, and the assay plate was covered and incubated for 2.5 h. After incubation, the solution was discarded, and the wells were washed four times with 300 μl of $1\times$ wash buffer using a multichannel pipette. After the last wash, the plate was inverted and blotted against clean paper towels for the complete removal of any remaining wash buffer by aspiration or decanting. Next, 100 μl of $1\times$ prepared biotinylated antibody was added to each well and incubated for 1 h, after which the solution was discarded and the washing step was repeated. A total of 100 μl of prepared streptavidin-HRP solution was added to each well and incubated for 45 min, after which the solution was discarded. The plate was then washed, and 100 μl of TMB substrate was added to each well and incubated for 30 min in the dark. Finally, 50 μl of stop solution was added to each well, and the absorbance was measured at 450 nm within 30 min of stopping the reaction. All incubations were performed at room temperature with gentle shaking, and all standards and samples were analyzed at least in duplicate.

Immunoprecipitation. Immunoprecipitation (IP) experiments were conducted according to a method reported previously (Bergman et al., 2004). WT and PS1 $2^{-/-}$ MEFs were seeded in 10 cm^2 dishes for 48 h and then lysed in 0.5 ml of coimmunoprecipitation buffer [50 mM HEPES, pH 7.4, 150 mM NaCl, 2 mM EDTA, Protease Inhibitor Mixture (catalog #11697498001, Roche), and 1% CHAPSO] followed by ultracentrifugation at 100,000 rpm for 20 min at 4°C . The samples were kept on ice and briefly sonicated before ultracentrifugation. The supernatants were then precleaned using protein G-Sepharose (Thermo Fisher Scientific) and subsequently immunoprecipitated overnight with goat anti-ApoE or normal goat IgG (dilution, 1:67), followed by end-over-end rotation. The following day, a mixture of protein G-Sepharose was added to the supernatants, and the incubation was continued for 3 h. The immunoprecipitates were then washed four times with coimmunoprecipitation buffer containing 0.5% CHAPSO and once in PBS, eluted using $4\times$ SDS sample buffer (250 mM Tris-HCl, pH 6.8, 40% glycerol, 8% SDS, and 0.01% bromophenol blue), heated at 95°C for 5 min, and analyzed by immunoblotting. For immunoblot blocking and antibody

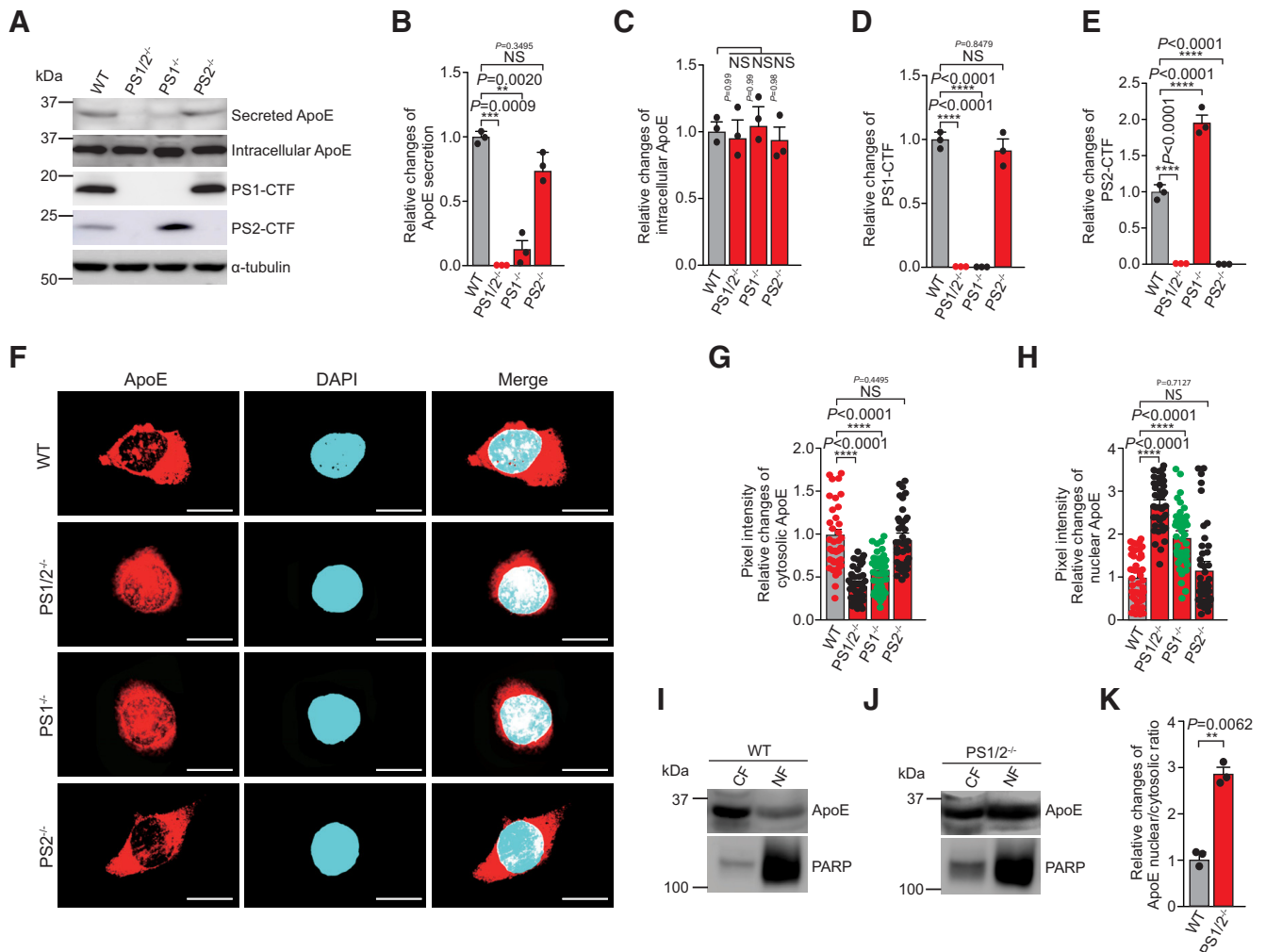


Figure 1. Lack of ApoE secretion and increased cytosol-to-nuclear translocation of ApoE in PS-deficient fibroblasts. **A**, Immunoblot analysis of ApoE secretion and intracellular ApoE, PS1-CTF, and PS2-CTF expression in WT, PS1/2^{-/-}, PS1^{-/-}, and PS2^{-/-} fibroblasts cultured for 48 h in serum-free medium. **B–E**, Quantification of ApoE secretion and intracellular ApoE, PS1-CTF, and PS2-CTF expression levels. Intracellular ApoE, PS1-CTF, and PS2-CTF expression levels were normalized to α -tubulin protein levels. $n = 3$. ** $p < 0.01$, *** $p < 0.001$, **** $p < 0.0001$. NS, Not significant, by one-way ANOVA followed by Tukey's multiple-comparison tests. **F**, Immunostaining for ApoE (red) and nuclear staining with DAPI (blue) in WT, PS1/2^{-/-}, PS1^{-/-}, and PS2^{-/-} fibroblasts. Scale bars, 5 μ m. **G**, **H**, Quantification of cytosolic and nuclear ApoE intensity in WT, PS1/2^{-/-}, PS1^{-/-}, and PS2^{-/-} fibroblasts. $n \geq 40$ different stained cells/group, nuclear boundaries determined based on DAPI. **** $p < 0.0001$. NS, Not significant, by one-way ANOVA followed by Tukey's multiple-comparison tests. **I, J**, Cytosolic and nuclear distribution of ApoE in WT and PS1/2^{-/-} fibroblasts. CF, Cytosolic fraction; NF, nuclear fraction. **K**, Quantification of ApoE nuclear/cytosolic ratio showed a significant increase in PS1/2^{-/-} fibroblasts compared with WT fibroblasts. $n = 3$. ** $p < 0.01$, by unpaired two-tailed t test. All quantitative data are shown as the mean \pm SEM. Formation of γ -secretase complex and cellular levels of NCT, PEN-2, and APh-1 in WT, PS1/2^{-/-}, PS1^{-/-}, and PS2^{-/-} fibroblasts are shown in Extended Data Figure 1-1.

incubation, 5% nonfat dry milk in TBS with Tween 20 (25 mM Tris-HCl, pH 8.0, 125 mM NaCl, and 0.5% Tween 20) was used. For immunoprecipitation, all steps were performed at 4°C.

Statistical analyses. Prism 7.0 software (GraphPad Software) was used for statistical analyses. All data are shown as the mean \pm SEM of at least three independent experiments with p values. $p < 0.05$ was considered statistically significant. Student's t tests were used to determine the significance of differences between two groups. Group differences were analyzed by one-way ANOVA followed by Tukey's multiple-comparison tests for multiple groups against the control group. All experiments produced similar results under identical or similar conditions, and the distribution of data were assumed to be normal.

Results

Lack of ApoE secretion and enhanced cytosol-to-nuclear translocation of ApoE in PS-deficient fibroblasts

Because not all PS mutations found in FAD can be interpreted by abnormal $A\beta$ generation, we hypothesized that PS may be involved in the pathogenesis of SAD and sought to identify its

function in regulating ApoE secretion. Notably, we found that ApoE secretion was completely abolished in PS1/2^{-/-} fibroblasts. PS1^{-/-} cells exhibited markedly reduced ApoE secretion, whereas PS2^{-/-} fibroblasts exhibited slightly reduced ApoE secretion compared with WT fibroblasts. Intracellular ApoE levels were not altered in these PS-deficient fibroblasts compared with WT fibroblasts (Fig. 1A–C). These results suggest that PS is essential for ApoE secretion but does not affect the levels of intracellular ApoE. The PS2-CTF levels in PS1^{-/-} cells were 1. Ninefold of those in WT cells (Fig. 1A,E). Formation of the PS2 γ -secretase complex was also dramatically upregulated in PS1^{-/-} fibroblasts compared with WT cells (Extended Data Fig. 1-1A,C); however, secreted ApoE was almost undetectable in the culture medium of PS1^{-/-} cells (Fig. 1A). These results suggest that PS1 or the PS1 γ -secretase complex is more crucial for ApoE secretion than PS2 or the PS2 γ -secretase complex.

To gain mechanistic insights into the lack of ApoE secretion by PS-deficient cells, we investigated whether the subcellular

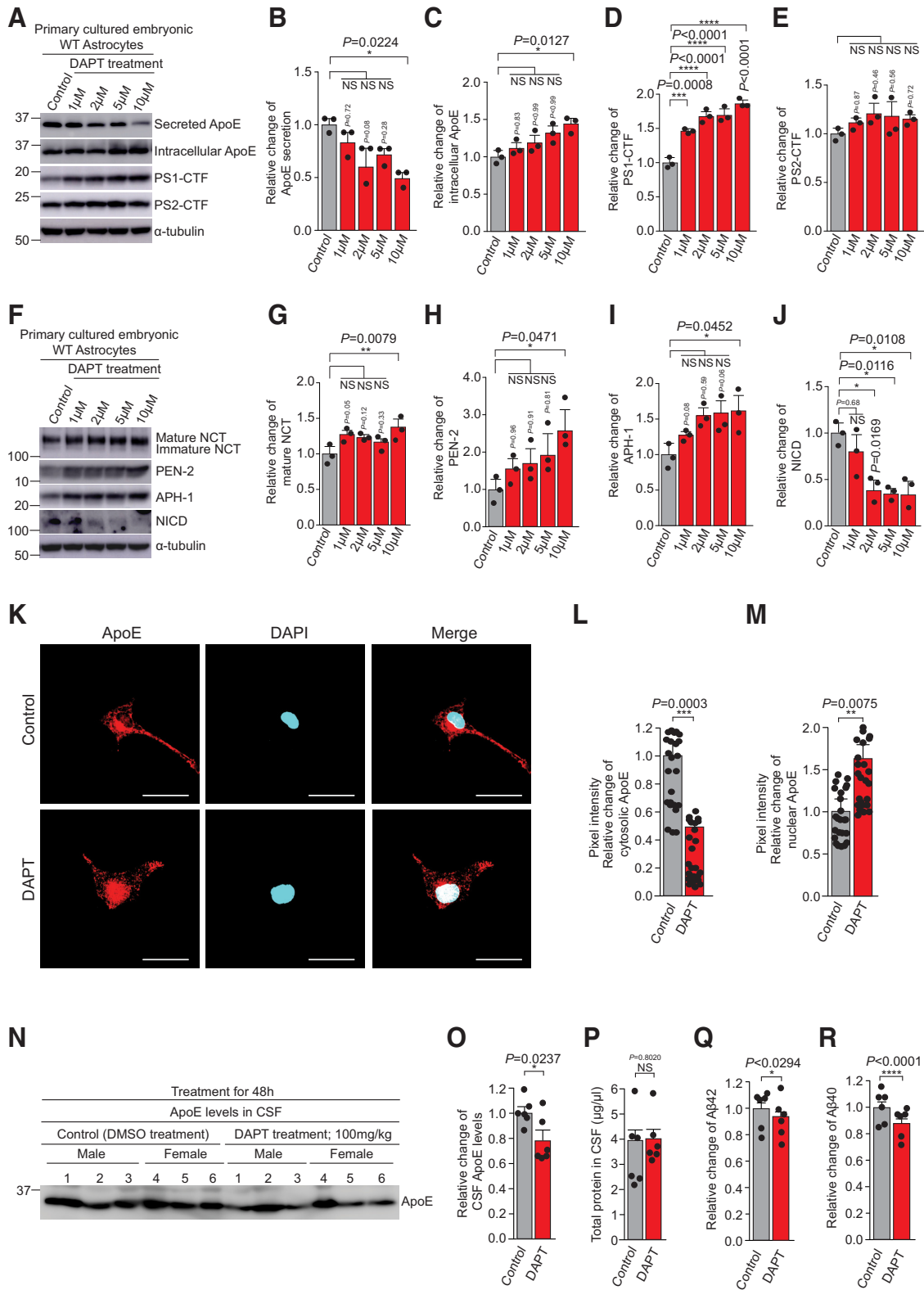


Figure 2. Inhibition of γ -secretase activity reduces ApoE secretion, promotes cytosol-to-nuclear translocation of ApoE in primary cultured embryonic WT astrocytes, and reduces ApoE levels in the CSF of DAPT-treated mice. **A**, Primary cultured embryonic WT astrocytes were treated with 1–10 μ M of DAPT or DMSO vehicle control for 48 h in serum-free conditional medium. Levels of secreted and intracellular ApoE, PS1-CTF, and PS2-CTF were determined by immunoblotting. **B–E**, Quantification of secreted and intracellular ApoE, PS1-CTF, and PS2-CTF levels from the experiment shown in **A**. $n = 3$; * $p < 0.05$, *** $p < 0.001$, **** $p < 0.0001$. NS, Not significant, by one-way ANOVA followed by Tukey's multiple-comparison tests. **F**, Immunoblot analysis of NCT, PEN-2, APH-1, and NICD in primary cultured embryonic WT astrocytes treated with DAPT. **G–J**, Quantification of mature NCT, PEN-2, APH-1, and NICD expression levels from the experiment shown in **F**, normalized to α -tubulin protein levels. **J**, Decreased NICD expression indicates inhibition of γ -secretase activity. $n = 3$; * $p < 0.05$, ** $p < 0.01$. NS, Not significant, by one-way ANOVA followed by Tukey's multiple-comparison tests. **K**, Immunostaining for cellular distribution of ApoE (red) and DAPI staining (nuclei, blue) in primary cultured embryonic WT astrocytes treated with DAPT for 24 h. Scale bars, 50 μ m. **L**, **M**, Quantification of cytosolic and nuclear ApoE intensity from the experiment shown in **K**. Cytosolic ApoE was significantly decreased and nuclear ApoE was significantly increased in 10 μ M of DAPT-treated astrocytes compared with control cells. $n \geq 24$ different stained cells/group. ** $p < 0.01$, *** $p < 0.001$, by unpaired

distribution of ApoE changed in these cells. We found that nuclear localization of ApoE was markedly enhanced by PS1 deficiency or PS1/2 deficiency. Correspondingly, cytosolic ApoE levels were dramatically lower in PS1/2^{-/-} and PS1^{-/-} fibroblasts compared with WT fibroblasts (Fig. 1F–H). We corroborated these findings through subcellular fractionation experiments. Nuclear fractionation was assessed by the presence of PARP, a nuclear marker. The nuclear/cytosolic ApoE ratio was 2.8-fold greater in PS1/2^{-/-} fibroblasts than in WT fibroblasts (Fig. 1I–K). These results suggest that abnormal nuclear translocation of ApoE in PS1/2^{-/-} and PS1^{-/-} cells may impair ApoE secretion.

We also measured the cellular levels of other γ -secretase components. As has been reported, depletion of both PS1 and PS2 completely abolished NCT maturation and PEN-2 cellular levels, whereas depletion of PS2 did not affect NCT maturation or PEN-2 levels, and PS2 deficiency caused only a strong reduction in APH-1 levels (Steiner et al., 2002; Zhang et al., 2005; Extended Data Fig. 1-1D–H).

Inhibition of γ -secretase activity reduces ApoE secretion *in vitro* and *in vivo*

Consistent with the findings in PS-deficient fibroblasts, we also found that blockade of γ -secretase activity using DAPT at 10 μ M significantly decreased ApoE secretion by both primary cultured embryonic WT astrocytes (Fig. 2A,B) and fibroblasts (Extended Data Fig. 2-1A,B). In contrast to PS1/2^{-/-} fibroblasts, the cellular levels of the γ -secretase components PS1-CTF, mature NCT, PEN-2, and APH-1 were significantly increased in DAPT-treated cells (Sogorb-Esteve et al., 2018; Fig. 2A,D,F–I, Extended Data Fig. 2-1A, D,F–I). Blockade of γ -secretase activity was confirmed by measuring A β levels and notch intracellular domain (NICD) generation (Fig. 2F,J, Extended Data Fig. 2-1F,J,N,O). Similar to PS1/2^{-/-} fibroblasts, the inhibition of γ -secretase activity significantly reduced cytosolic ApoE levels and increased those of nuclear ApoE (Fig. 2K–M, Extended Data Fig. 2-1K–M). These results strongly suggest that ApoE secretion depends on γ -secretase activity, regardless of the levels of the proteins that constitute this activity. The *in vivo* effects of γ -secretase inhibition were examined by treating WT mice with DAPT via intraperitoneal injection. ApoE levels in CSF were significantly decreased in DAPT-treated mice compared with control mice (Fig. 2N,O). Total protein in CSF did not show any change in DAPT-treated mice compared with control mice (Fig. 2P). A β 40 and A β 42 levels in the cortex of DAPT-treated mice were also significantly decreased compared with control mice (Fig. 2Q,R). These results suggest that decreased γ -secretase activity reduces ApoE secretion *in vivo*.

Reduced ApoE secretion in NCT^{-/-} fibroblasts

Because PS1 has multiple functions in addition to γ -secretase activity (Donoviel et al., 1999), we investigated whether the loss of

γ -secretase activity impaired ApoE secretion in NCT^{-/-} fibroblasts. We also found that ApoE secretion significantly decreased, but was not completely abolished, in NCT^{-/-} fibroblasts (Fig. 3A,B), possibly because PS1-CTF and the γ -secretase complex (PS1 and APH-1) were still present (Fig. 3A,D,J,K,N) and γ -secretase activity was still detectable in these cells (Li et al., 2003b). NCT deficiency also resulted in a decrease in the molecular weight of both secreted and intracellular ApoE (Fig. 3A), suggesting that NCT is involved in O-linked glycosylation of ApoE (Wernette-Hammond et al., 1989; Flowers et al., 2020). We also confirmed that NCT deficiency dramatically reduced NICD generation and the levels of PEN-2 and APH-1 (Zhao et al., 2010; Fig. 3F–I). Similar to PS-deficient cells, cytosolic ApoE levels significantly decreased and nuclear ApoE levels significantly increased in NCT^{-/-} fibroblasts compared with WT fibroblasts (Fig. 3O–Q). These results suggest that the loss of γ -secretase activity increases abnormal translocation of ApoE from the cytosol to the nucleus and impairs ApoE secretion.

Fully restoration of ApoE secretion by WT PS1 but not by PS1 mutants in PS1/2^{-/-} fibroblasts

We also examined whether PS1 expression restores ApoE secretion in PS1/2^{-/-} fibroblasts. PS1/2^{-/-} fibroblasts were infected with retrovirus vectors expressing human WT PS1 or human PS1 bearing FAD-associated mutations (PS1 Δ E9, PS1L166P, or PS1G384A). WT PS1 restored ApoE secretion in PS1/2^{-/-} fibroblasts to a level similar to that of WT fibroblasts, whereas PS1 Δ E9, PS1L166P, and PS1G384A PS1 mutants restored ApoE secretion to a lesser degree than WT PS1 (Fig. 4A,B). After infection with the retrovirus vectors, the similarity of levels of WT PS1 and PS1 mutants in PS1/2^{-/-} fibroblasts was confirmed (Fig. 4A). Instead of PS1-CTF, full-length PS1 was detected in PS1/2^{-/-} cells infected with PS1 Δ E9, because PS1 Δ E9 lacks an exon-containing endocleavage site (Steiner et al., 1999). WT PS1 dramatically restored the cytosolic localization of ApoE in PS1/2^{-/-} fibroblasts, whereas the PS1 Δ E9, PS1L166P, and PS1G384A PS1 mutants exhibited no significant effects (Fig. 4C,D). We also found that WT PS1 restored ApoE secretion and increased cytosolic localization of ApoE in PS1/2^{-/-} fibroblasts in a dose-dependent manner accompanied by reduced nuclear localization of ApoE (Extended Data Fig. 4-1), suggesting that ApoE secretion is positively correlated with WT PS1 levels and cytosolic localization of ApoE.

We also examined whether PS1 or PS2 mutants exert a dominant-negative effect on ApoE secretion in primary cultured embryonic ApoE3-KI fibroblasts, which secrete more ApoE than normal WT fibroblasts. Overexpression of WT PS1 increased ApoE secretion and cytosolic ApoE localization, accompanied by decreased nuclear localization of ApoE (Extended Data Fig. 4-2A,B,F–H). However, PS1 Δ E9, PS1L166P, PS1G384A, WT PS2, and PS2N141I exhibited no significant effect on ApoE secretion or the subcellular localization of ApoE in ApoE3-KI fibroblasts (Extended Data Fig. 4-2A,B,F–H,I,J,N–P). These results suggest that if WT PS or γ -secretase activity persists at normal levels, PS mutations would have no dominant-negative effect on ApoE secretion, and that WT PS1 has stronger effects in promoting ApoE secretion and its cytosolic localization than WT PS2.

Reduced plasma ApoE levels in FAD patients carrying PS1 mutations compared with normal control subjects

To determine whether reduced γ -secretase activity affects ApoE levels *in vivo*, we investigated ApoE levels in human plasma from FAD patients carrying PS1 mutations and age-matched healthy control subjects. Previous reports showed that these PS1 mutations

←

two-tailed *t* tests. **N**, Western blot analysis of ApoE levels in CSF from WT C57BL/6J mice treated with DAPT or DMSO vehicle control. **O**, Quantification of CSF ApoE levels from the experiment shown in **N**. DAPT treatment significantly decreased CSF ApoE levels in WT C57BL/6J mice compared with control mice. *n* = 6 mice/group. **p* < 0.05, by unpaired two-tailed *t* test. **P**, Quantification of total protein in CSF. *n* = 6 mice/group. NS, Not significant, by unpaired two-tailed *t* test. **Q, R**, A β 40 and A β 42 levels in the cortex of mice measured using an A β 40 or A β 42 ELISA kit. **P, Q**, DAPT treatment significantly decreased the levels of A β 42 (**P**) and A β 40 (**Q**). *n* = 6 mice/group. **p* < 0.05, *****p* < 0.0001, by unpaired two-tailed *t* test. All quantitative data shown as the mean \pm SEM. Primary cultured embryonic WT fibroblasts were also treated with DAPT, and similar results are shown in Extended Data Figure 2-1.

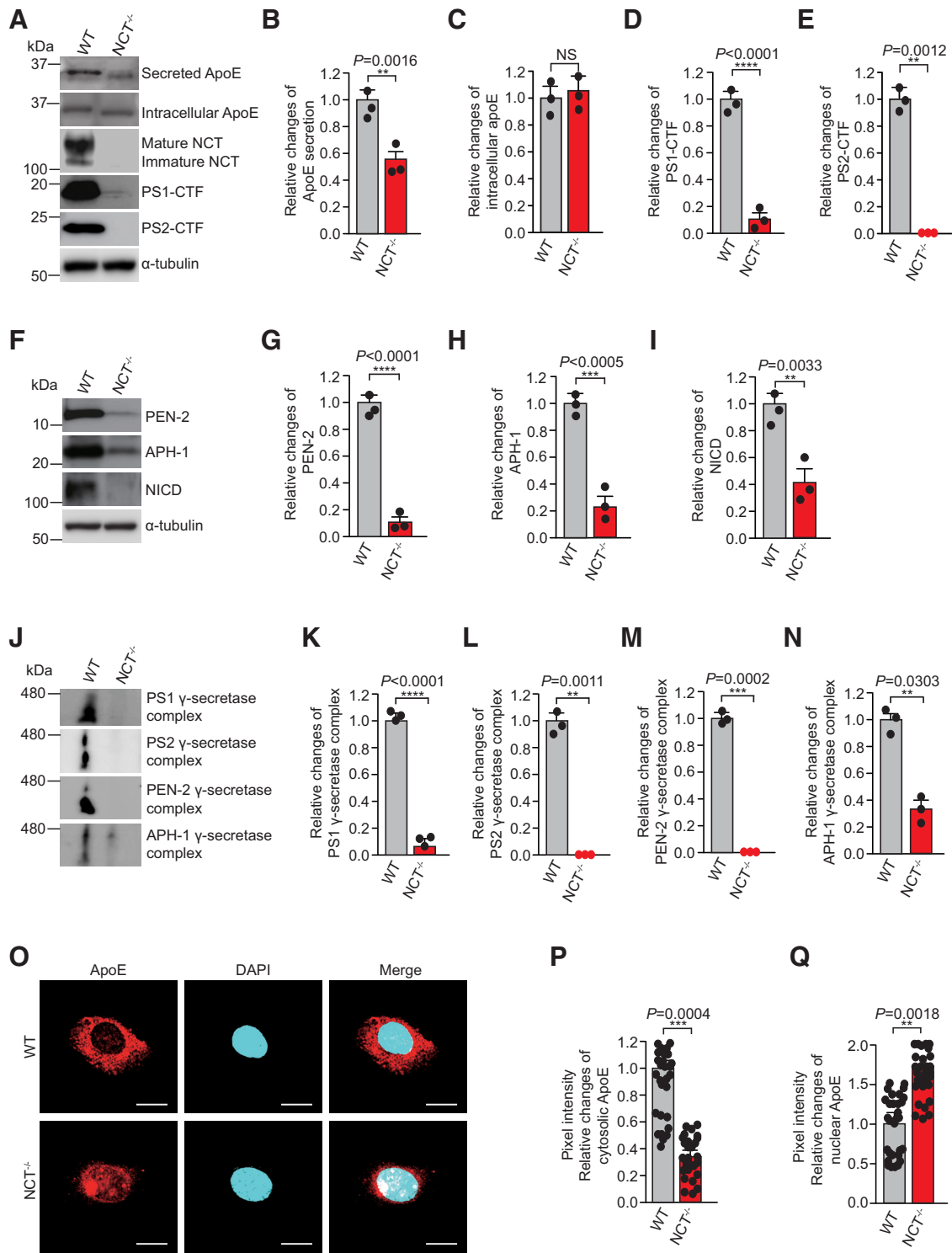


Figure 3. Reduced ApoE secretion and increased cytosol-to-nuclear translocation of ApoE in NCT^{-/-} fibroblasts. **A**, Immunoblot analysis of secreted and intracellular ApoE, NCT, PS1, and PS2 in WT and NCT^{-/-} fibroblasts. **B–E**, Quantification of secreted ApoE, intracellular ApoE, PS1-CTF, and PS2-CTF expression levels shown in **A**. **B, D**, ApoE secretion and PS1-CTF levels were significantly decreased in NCT^{-/-} fibroblasts. Intracellular ApoE, PS1-CTF, and PS2-CTF expression levels were normalized to α-tubulin protein levels. *n* = 3. *****p* < 0.01**, *******p* < 0.0001**. NS, Not significant, by unpaired two-tailed *t* test. **F**, Immunoblot analysis of PEN-2, APH-1, and NICD levels in WT and NCT^{-/-} fibroblasts. **G–I**, Quantification of the levels of PEN-2, APH-1, and NICD from the experiment shown in **F**. Levels of PEN-2, APH-1, and NICD were significantly decreased in NCT^{-/-} fibroblasts compared with WT fibroblasts. PEN-2, APH-1, and NICD expression levels were normalized to α-tubulin protein levels. *n* = 3. *****p* < 0.01**, ******p* < 0.001**, *******p* < 0.0001**, by unpaired two-tailed *t* test. **J**, A total of 5 μg of protein from cell lysates of WT and NCT^{-/-} fibroblasts was subjected to Blue native PAGE (BN-PAGE) and analyzed by immunoblotting using PS1-CTF, PS2-CTF, PEN-2, and APH-1 antibodies. **K–N**, Quantification of PS1, PS2, PEN-2, and APH-1 γ-secretase complex formation from the experiment shown in **J**. PS1 and APH-1 γ-secretase complex formation was significantly decreased in NCT^{-/-} fibroblasts compared with WT cells. *n* = 3. *****p* < 0.01**, ******p* < 0.001**, *******p* < 0.0001**, by unpaired two-tailed *t* test. **O**, Immunostaining for cellular distribution of ApoE (red) and DAPI staining (nuclei, blue) in WT and NCT^{-/-} fibroblasts. Scale bars, 10 μm. **P, Q**, Quantification of cytosolic and nuclear fluorescence intensity from the experiment shown in **O**. Cytosolic ApoE was significantly decreased and nuclear ApoE significantly increased in NCT^{-/-} fibroblasts compared with WT fibroblasts. Nuclear boundaries were determined based on DAPI. *n* = 20 different stained cells/group, *****p* < 0.01**, ******p* < 0.001**, by unpaired two-tailed *t* test. All data are shown as the mean ± SEM.

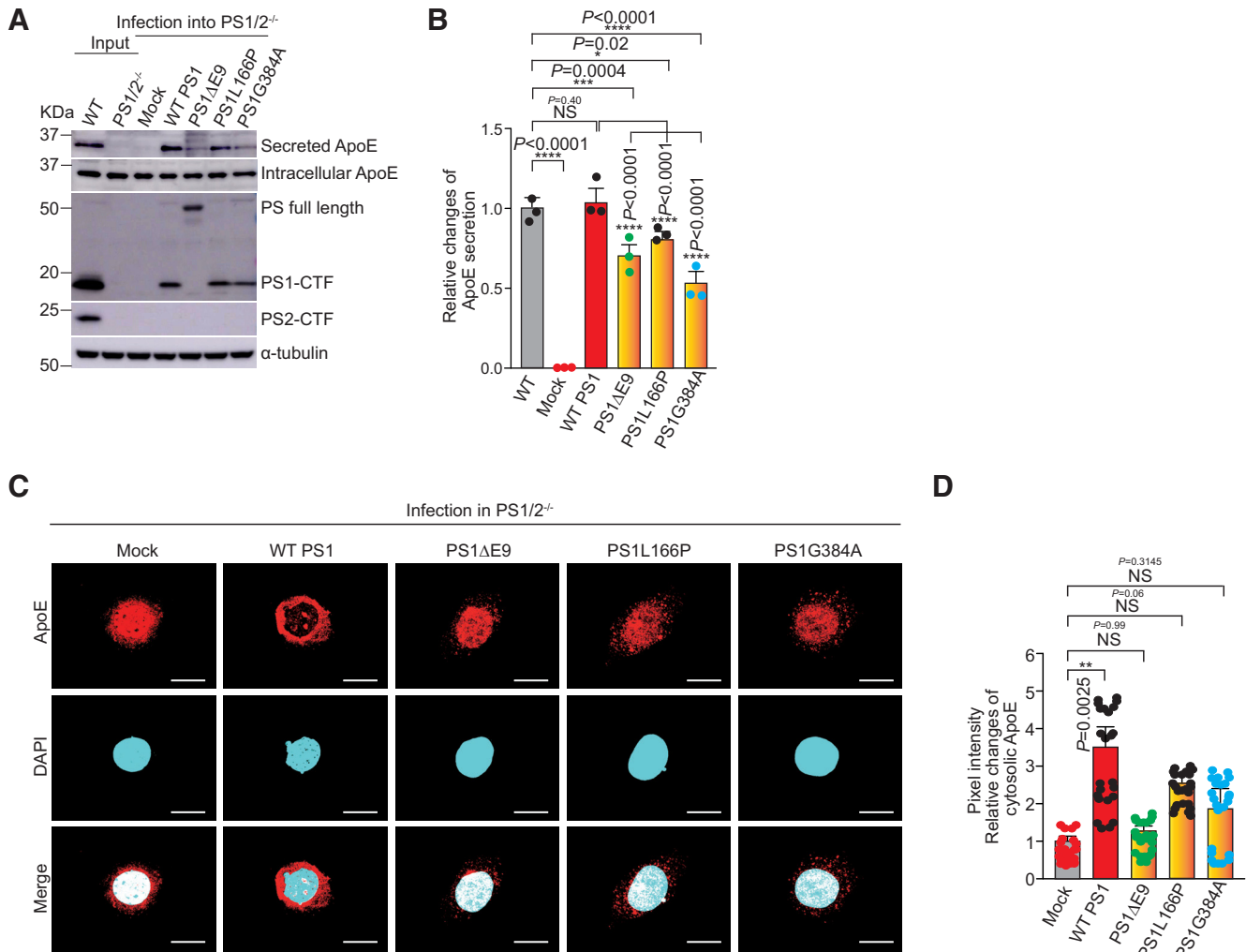


Figure 4. Human PS1 bearing FAD mutations restored from ApoE secretion to a lesser degree than WT PS1. **A**, Immunoblot analysis of secreted and intracellular ApoE, PS1, and PS2 in WT fibroblasts and PS1/2^{-/-} fibroblasts infected with retrovirus vectors bearing human WT PS1 or PS1 with FAD mutations (PS1ΔE9, PS1L166P, and PS1G384A). **B**, Quantification of secreted ApoE levels. The level of ApoE secreted from WT fibroblasts was adjusted to 1. $n = 3$. * $p < 0.05$, *** $p < 0.001$, **** $p < 0.0001$. NS, Not significant, by one-way ANOVA followed by Tukey's multiple-comparison tests. **C**, Confocal microscopy analysis of cytosolic and nuclear localization of ApoE. Nuclei were stained with DAPI. Scale bars, 2 μm . **D**, Quantification of cytosolic intensity of ApoE shown in **C**. WT PS significantly restored the cytosolic distribution of ApoE in PS1/2^{-/-} fibroblasts, whereas PS1ΔE9, PS1L166P, and PS1G384A did not show significant restoration. $n = 20$ different stained cells/group. ** $p < 0.01$. NS, Not significant, by one-way ANOVA followed by Tukey's multiple-comparison tests. All quantitative data are shown as the mean \pm SEM. Overexpression of WT PS1 enhanced ApoE secretion in PS1/2^{-/-} fibroblasts and primary cultured embryonic ApoE3-KI fibroblasts (Extended Data Figures 4-1, 4-2).

result in decreased or altered γ -secretase activity (Jørgensen et al., 1996; Yasuda et al., 1999; Hamaguchi et al., 2009; Liu et al., 2017; Sun et al., 2017). There was no significant difference in mean age between the FAD patients (51.04 ± 2.30 years) and controls (55.58 ± 1.96 years; $p = 0.1469$). Plasma ApoE levels in FAD patients with PS1 mutations were significantly reduced compared with healthy control subjects (Fig. 5A). There was no significant correlation between plasma ApoE level and age among the control, PS1 mutation, and combined groups (Fig. 5B–D). These results suggest that decreased γ -secretase activity induced by PS1 mutations negatively regulates ApoE secretion.

PS deficiency increases binding of importin $\alpha 4$ to ApoE and enhances nuclear colocalization of importin $\alpha 4$ /ApoE in PS1/2^{-/-} fibroblasts

The importin α family of multipurpose nuclear transport receptors mediate the nuclear translocation of many proteins, including NICD, signal transducer and activator of transcription 1 (STAT1), and STAT2 (Goldfarb et al., 2004; Huenniger et al.,

2010). Importin $\alpha 4$ exhibits the strongest affinity for NICD, whereas importin $\alpha 3$ exhibits moderate affinity for NICD (Huenniger et al., 2010). Interestingly, levels of importin $\alpha 4$, but not of importin $\alpha 3$, were significantly increased in PS1/2^{-/-} fibroblasts in the present study, and NICD generation was completely abolished in PS1/2^{-/-} fibroblasts (Fig. 6A–D). We then examined potential interactions between importin $\alpha 3$ or $\alpha 4$ and ApoE using IP assays and found that importin $\alpha 4$, but not importin $\alpha 3$, bound to ApoE. In addition, ApoE bound more importin $\alpha 4$ in PS1/2^{-/-} fibroblasts than in WT fibroblasts (Fig. 6E,F). Confocal microscopy studies demonstrated that the colocalization of importin $\alpha 4$ and ApoE was significantly higher in the nucleus of PS1/2^{-/-} fibroblasts (Fig. 6G,H). These results suggest that nuclear transport of ApoE is mediated by importin $\alpha 4$ and may be enhanced by the lack of NICD in PS1/2^{-/-} cells.

Discussion

Abnormal A β generation and an increased A β 42/A β 40 ratio induced by PS1 mutations have long been considered causative

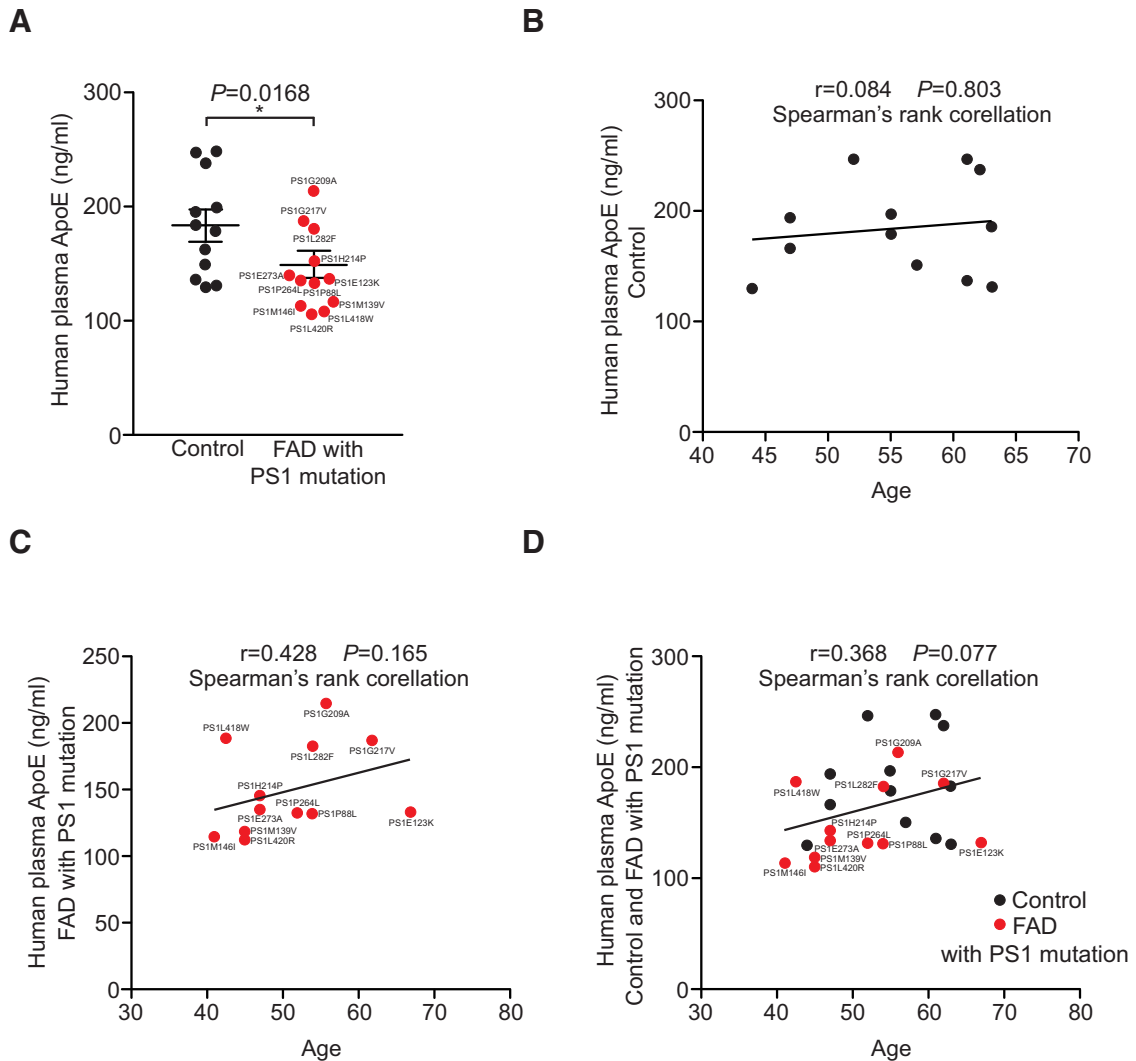


Figure 5. Reduced ApoE levels in the plasma of FAD patients carrying pathogenic PS1 mutations. **A**, ApoE levels in plasma of control individuals and FAD patients carrying PS1 mutations were determined using an ELISA kit. Plasma ApoE levels were significantly lower in FAD patients with PS1 mutations than control subjects. Control subjects, $n = 12$; FAD patients, $n = 12$. $*p < 0.05$, by unpaired two-tailed t test. **B–D**, There was no statistically significant correlation between plasma ApoE level and age. p -Values were determined by Spearman rank test. All data are shown as the mean \pm SEM.

factors for FAD (Sun et al., 2017). Here, we demonstrated a novel function of PS; that is, PS is essential for ApoE secretion, and decreased γ -secretase activity induced by PS mutations reduces ApoE secretion. We demonstrated that PS-deficient cells completely abolished ApoE secretion. Furthermore, we showed that the blockade of γ -secretase activity by a γ -secretase inhibitor, DAPT, decreased ApoE secretion both in astrocytes and in CSF, suggesting that γ -secretase activity is crucial for ApoE secretion in brain. A mature γ -secretase consists of the following four components: PS, NCT, APH-1, and PEN-2. These four core components of the γ -secretase complex tightly regulate each other's expression, maturation, and assembly as well as γ -secretase activity (Takasugi et al., 2003; Capell et al., 2005). To corroborate the involvement of other γ -secretase molecule, we demonstrated that NCT deficiency reduced ApoE secretion, but its secretion was not completely abolished, possibly because PS function or γ -secretase activity was still present in NCT-deficient cells. These results suggest that NCT partially regulates ApoE secretion and PS plays the key role in ApoE secretion. We also observed an altered post-translational modification of ApoE in NCT-deficient cells (Fig. 3A). Relatedly, an aberrant migration

of ApoE was also found in the intracellular fraction of PS1^{-/-} cells (Fig. 1A). Previous study reported that NCT is required for processing and trafficking of APP in mammals and secretion of A β peptides is abolished in NCT-deficient fibroblasts, suggesting a role of NCT in secretory pathway (Li et al., 2003a). Glycosylation occurs in endoplasmic reticulum-to-Golgi apparatus very early in the secretory pathway. Nonetheless, the role of NCT and PS deficiency in ApoE glycosylation in the secretory pathway needs further investigation.

PS mutations lead to the loss of function of γ -secretase, which was confirmed by decreased cleavage of Notch, syndecan, and N-cadherin, and this can probably be extended to other substrates (De Strooper, 2007). Importantly, FAD patients carrying pathogenic PS1 mutations exhibited lower plasma ApoE levels than control subjects. In contrast to the changes in A β generation associated with FAD, decreased A β clearance is crucial for the pathogenesis of SAD, and ApoE plays a major role in brain A β clearance (Scheltens et al., 2016). For example, SAD patients carrying the ApoE4 allele show decreased A β clearance in the CSF compared with carriers of ApoE3 or ApoE2 allele (Castellano et al., 2011; Yamazaki et al., 2019). Together, these

findings suggest that loss of PS function alters the generation of A β and impairs ApoE secretion, both of which may initiate and accelerate A β accumulation, ultimately leading to the development of AD.

PS associated with the trafficking of various proteins, including NCT, APP, triggering receptor expressed on myeloid cells 2, integrin β 1, and ApoE receptor 2 (Zou et al., 2008; De Strooper et al., 2012). Our results suggest that PS or γ -secretase components may also be involved in ApoE trafficking; however, γ -secretase activity, regardless of the levels of γ -secretase components, is crucial for ApoE secretion (Fig. 2A,B,D,F–I, Extended Data Fig. 2-1A,B,D,F–I). ApoE is a 34 kDa glycoprotein that is highly expressed and secreted by various cell types (Hasel and Liddelov, 2021). Although ApoE is predominantly present in the cytosol, its presence in the nuclear compartment has also been reported (Theendakara et al., 2016). A recent study demonstrated that both ApoE3 and ApoE4 bound to SirT1 promoter sequence in the nucleus with similar binding affinities and downregulated the transcription of SirT1, a predominantly nuclear protein. In addition to the overall reduction in SirT1 protein expression, only ApoE4 caused the redistribution of SirT1 from the nucleus to the cytosol (Theendakara et al., 2016). The nuclear roles of ApoE are given additional significance with the demonstrations that ApoE4 specifically binds certain DNA sequences, namely “CLEAR” (coordinated lysosomal expression and regulation) elements. This connects the phenomenon of nuclear ApoE to negative outcomes, specifically the growing interest in autophagic failure in AD (Parcon et al., 2018; Lima et al., 2020). Furthermore, ApoEs are shown to be associated with the transcription of MADD (MAP kinase-activating death domain) and COMMD6 genes, which further bind to the nuclear factor- κ B complex or the RelA subunit of the complex to regulate transcription (Del Villar and Miller, 2004; de Bie et al., 2006; Theendakara et al., 2016). These findings suggest that ApoE can translocate to the nucleus and recycle back to the cytosol. However, the mechanism by which ApoE escapes the secretory pathway and translocates to the nucleus from cytosol is currently unclear. Importin α family proteins are multipurpose nuclear transport receptors that bind to hundreds of proteins, including NICD, linking them to importin β to facilitate their translocation from the cytosol to the nucleus (Goldfarb et al., 2004; Huenniger et al., 2010). Here, we report that ApoE

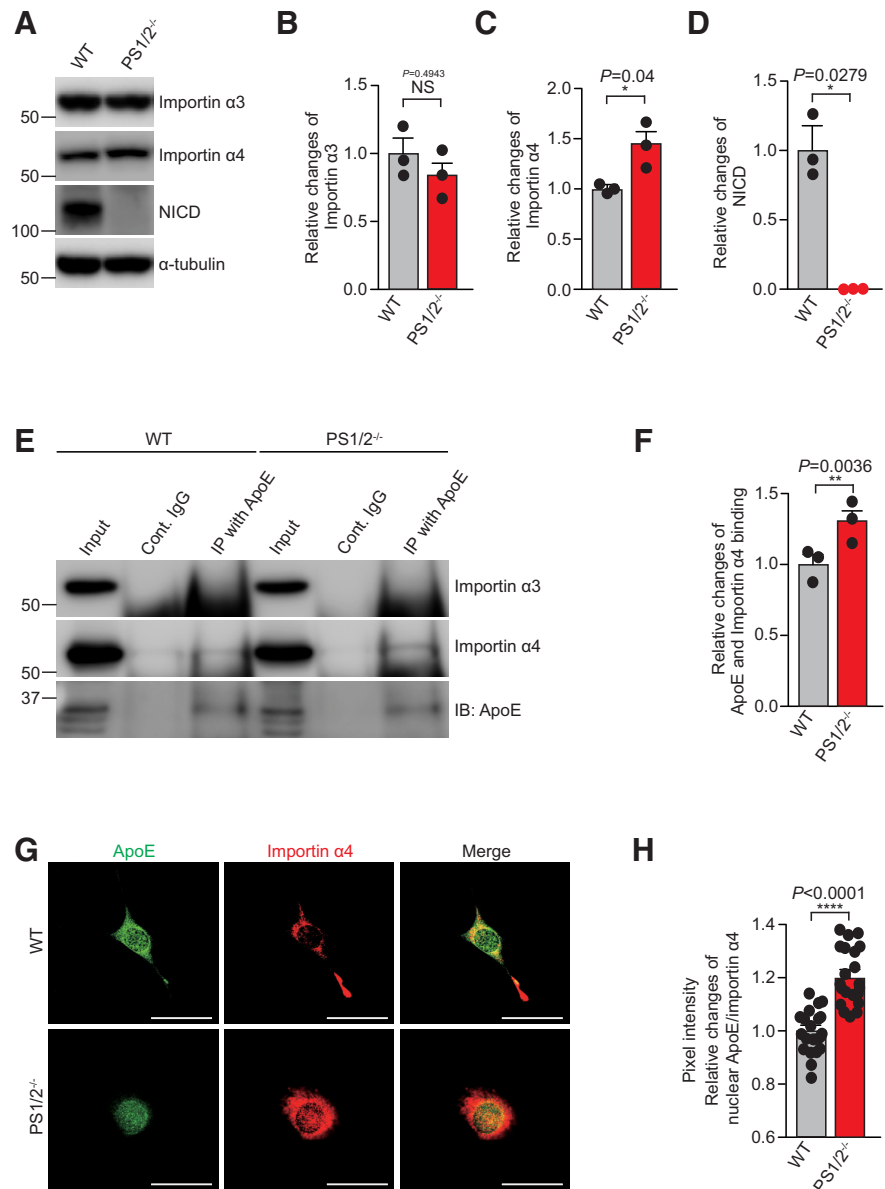


Figure 6. Increased binding of importin α 4 to ApoE and enhanced nuclear colocalization of importin α 4/ApoE in PS1/2^{-/-} fibroblasts. **A**, Immunoblot analysis of importin α 3, importin α 4, and NICD in WT and PS1/2^{-/-} fibroblasts cultured for 48 h. **B–D**, Quantification of importin α 3, importin α 4, and NICD levels from the experiments shown in **A**, normalized to α -tubulin protein levels. $n = 3$. * $p < 0.05$. NS, Not significant, by unpaired two-tailed t test. **E**, **F**, Immunoprecipitation analysis of the binding of ApoE to importin α 3 or importin α 4. ApoE bound more importin α 4 in PS1/2^{-/-} fibroblasts than in WT fibroblasts. $n = 3$. ** $p < 0.01$, by unpaired two-tailed t test. **G**, Immunostaining analysis showed that importin α 4 colocalized with ApoE in the cytosol of WT fibroblasts, whereas the colocalization was found predominantly in the nucleus of PS1/2^{-/-} fibroblasts. Scale bars, 50 μ m. WT and PS1/2^{-/-} fibroblasts were stained with secondary antibodies labeled with Alexa Fluor 488 and Alexa Fluor 568: ApoE (green), importin α 4 (red). **H**, Quantification of fluorescence intensity of colocalized ApoE/importin α 4 in nucleus from the experiment shown in **G**. $n = 21$ different stained cells/group. **** $p < 0.0001$, by unpaired two-tailed t test. All quantitative data are shown as the mean \pm SEM.

binds to importin α 4 to facilitate the translocation of ApoE from the cytosol to the nucleus in PS-deficient cells, suggesting that abnormal translocation of ApoE from the cytosol to the nucleus attenuates ApoE secretion. ApoE has been shown to be a transcriptional regulator of many genes that are potentially involved in AD (Theendakara et al., 2016). Although the significance of the enhanced nuclear localization of ApoE in PS-deficient cells is not clear, it is possible that enhanced nuclear ApoE may suppress or activate the transcription of some genes that are regulated by PS or NICD.

Together, this study demonstrated a novel link of PS to ApoE, tying together the mechanisms associated with FAD and SAD. PS mutations and ApoE4 have long been considered to cause FAD and SAD by two independent mechanisms, abnormal A β generation and impaired A β clearance, respectively. For the first time, we demonstrated that PS is essential for the secretion of ApoE, suggesting that PS mutations or altered γ -secretase activity is also involved in A β clearance via regulation of ApoE secretion. Our findings may offer opportunities for the development of novel AD treatment targets.

References

- Abdullah M, Kimura N, Akatsu H, Hashizume Y, Ferdous T, Tachita T, Iida S, Zou K, Matsubara E, Michikawa M (2019) Flotillin is a novel diagnostic blood marker of Alzheimer's disease. *J Alzheimers Dis* 72:1165–1176.
- Bai XC, Yan C, Yang G, Lu P, Ma D, Sun L, Zhou R, Scheres SHW, Shi Y (2015) An atomic structure of human γ -secretase. *Nature* 525:212–217.
- Bergman A, Laudon H, Winblad B, Lundkvist J, Näslund J (2004) The extreme C terminus of presenilin 1 is essential for γ -secretase complex assembly and activity. *J Biol Chem* 279:45564–45572.
- Borchelt DR, Thinakaran G, Eckman CB, Lee MK, Davenport F, Ratovitsky T, Prada C-M, Kim G, Seekins S, Yager D, Slunt HH, Wang R, Seeger M, Levey AI, Gandy SE, Copeland NG, Jenkins NA, Price DL, Younkin SG, Sisodia SS (1996) Familial Alzheimer's disease-linked presenilin 1 variants elevate A β 1-42/1-40 ratio in vitro and in vivo. *Neuron* 17:1005–1013.
- Capell A, Behr D, Prokop S, Steiner H, Kaether C, Shearman MS, Haass C (2005) γ -secretase complex assembly within the early secretory pathway. *J Biol Chem* 280:6471–6478.
- Castellano JM, Kim J, Stewart FR, Jiang H, DeMattos RB, Patterson BW, Fagan AM, Morris JC, Mawuenyega KG, Cruchaga C, Goate AM, Bales KR, Paul SM, Bateman RJ, Holtzman DM (2011) Human apoE isoforms differentially regulate brain amyloid-beta peptide clearance. *Sci Transl Med* 3:89ra57.
- Comery TA, Martone RL, Aschmies S, Atchison KP, Diamantidis G, Gong X, Zhou H, Kreft AF, Pangalos MN, Sonnenberg-Reines J, Jacobsen JS, Marquis KL (2005) Acute γ -secretase inhibition improves contextual fear conditioning in the Tg2576 mouse model of Alzheimer's disease. *J Neurosci* 25:8898–8902.
- de Bie P, van de Sluis B, Burstein E, Duran Karen J, Berger R, Duckett Colin S, Wijmenga C, Klomp LWJ (2006) Characterization of COMMD protein-protein interactions in NF- κ B signalling. *Biochem J* 398:63–71.
- Del Villar K, Miller CA (2004). Down-regulation of DENN/MADD, a TNF receptor binding protein, correlates with neuronal cell death in Alzheimer's disease brain and hippocampal neurons. *Proc Natl Acad Sci U S A* 101:4210.
- De Strooper B (2007) Loss-of-function presenilin mutations in Alzheimer disease. *Talking Point on the role of presenilin mutations in Alzheimer disease*. *EMBO Rep* 8:141–146.
- De Strooper B, Iwatsubo T, Wolfe MS (2012) Presenilins and gamma-secretase: structure, function, and role in Alzheimer Disease. *Cold Spring Harb Perspect Med* 2 a006304.
- Donoviel DB, Hadjantonakis AK, Ikeda M, Zheng H, Hyslop PS, Bernstein A (1999) Mice lacking both presenilin genes exhibit early embryonic patterning defects. *Genes Dev* 13:2801–2810.
- Duggan SP, McCarthy JV (2016) Beyond γ -secretase activity: the multifunctional nature of presenilins in cell signalling pathways. *Cell Signal* 28:1–11.
- Fagan AM, Watson M, Parsadanian M, Bales KR, Paul SM, Holtzman DM (2002) Human and murine ApoE markedly alters A β metabolism before and after plaque formation in a mouse model of Alzheimer's disease. *Neurobiol Dis* 9:305–318.
- Flowers SA, Grant OC, Woods RJ, Rebeck GW (2020) O-glycosylation on cerebrospinal fluid and plasma apolipoprotein E differs in the lipid-binding domain. *Glycobiology* 30:74–85.
- Futai E, Osawa S, Cai T, Fujisawa T, Ishiura S, Tomita T (2016) Suppressor mutations for presenilin 1 familial Alzheimer disease mutants modulate γ -secretase activities. *J Biol Chem* 291:435–446.
- Golde TE, Estus S, Younkin LH, Selkoe DJ, Younkin SG (1992) Processing of the amyloid protein precursor to potentially amyloidogenic derivatives. *Science* 255:728–730.
- Goldfarb DS, Corbett AH, Mason DA, Harreman MT, Adam SA (2004) Importin α : a multipurpose nuclear-transport receptor. *Trends Cell Biol* 14:505–514.
- Gong J-S, Kobayashi M, Hayashi H, Zou K, Sawamura N, Fujita SC, Yanagisawa K, Michikawa M (2002) Apolipoprotein E (ApoE) isoform-dependent lipid release from astrocytes prepared from human ApoE3 and ApoE4 knock-in mice. *J Biol Chem* 277:29919–29926.
- Hamaguchi T, Morinaga A, Tsukie T, Kuwano R, Yamada M (2009) A novel presenilin 1 mutation (L282F) in familial Alzheimer's disease. *J Neurol* 256:1575–1577.
- Hasel P, Liddel SA (2021) Isoform-dependent APOE secretion modulates neuroinflammation. *Nat Rev Neurol* 17:265–266.
- Herreman A, Hartmann D, Annaert W, Saftig P, Craessaerts K, Serneels L, Umans L, Schrijvers V, Checler F, Vanderstichele H, Baekelandt V, Dressel R, Cupers P, Huylebroeck D, Zwijsen A, Van Leuven F, De Strooper B (1999) Presenilin 2 deficiency causes a mild pulmonary phenotype and no changes in amyloid precursor protein processing but enhances the embryonic lethal phenotype of presenilin 1 deficiency. *Proc Natl Acad Sci U S A* 96:11872–11877.
- Holtzman DM, Bales KR, Tenkova T, Fagan AM, Parsadanian M, Sartorius LJ, Mackey B, Olney J, McKeel D, Wozniak D, Paul SM (2000) Apolipoprotein E isoform-dependent amyloid deposition and neuritic degeneration in a mouse model of Alzheimer's disease. *Proc Natl Acad Sci U S A* 97:2892–2897.
- Huang Y, Mucke L (2012) Alzheimer mechanisms and therapeutic strategies. *Cell* 148:1204–1222.
- Huenniger K, Krämer A, Soom M, Chang I, Köhler M, Depping R, Kehlenbach RH, Kaether C (2010) Notch1 signaling is mediated by importins alpha 3, 4, and 7. *Cell Mol Life Sci* 67:3187–3196.
- Isobe I, Michikawa M, Yanagisawa K (1999) Enhancement of MTT, a tetrazolium salt, exocytosis by amyloid β -protein and chloroquine in cultured rat astrocytes. *Neurosci Lett* 266:129–132.
- Jørgensen P, Bus C, Pallisgaard N, Bryder M, Jørgensen AL (1996) Familial Alzheimer's disease co-segregates with a Met146Ile substitution in presenilin-1. *Clin Genet* 50:281–286.
- Kanekiyo T, Xu H, Bu G (2014) ApoE and A β in Alzheimer's disease: accidental encounters or partners? *Neuron* 81:740–754.
- Kimberly WT, LaVoie MJ, Ostaszewski BL, Ye W, Wolfe MS, Selkoe DJ (2003) γ -secretase is a membrane protein complex comprised of presenilin, nicastrin, Aph-1, and Pen-2. *Proc Natl Acad Sci U S A* 100:6382–6387.
- Kitamura T, Koshino Y, Shibata F, Oki T, Nakajima H, Nosaka T, Kumagai H (2003) Retrovirus-mediated gene transfer and expression cloning: powerful tools in functional genomics. *Exp Hematol* 31:1007–1014.
- Li T, Ma G, Cai H, Price DL, Wong PC (2003a) Nicastrin is required for assembly of presenilin/ γ -secretase complexes to mediate Notch signaling and for processing and trafficking of β -amyloid precursor protein in mammals. *J Neurosci* 23:3272–3277.
- Li J, Fici GJ, Mao C-A, Myers RL, Shuang R, Donoho GP, Pauley AM, Himes CS, Qin W, Kola I, Merchant KM, Nye JS (2003b) Positive and negative regulation of the γ -secretase activity by nicastrin in a murine model. *J Biol Chem* 278:33445–33449.
- Li Z (2019) New APOE-related therapeutic options for Alzheimer's disease. *AIP Conf Proc* 2058:020002.
- Lima D, Hacke ACM, Inaba J, Pessôa CA, Kerman K (2020) Electrochemical detection of specific interactions between apolipoprotein E isoforms and DNA sequences related to Alzheimer's disease. *Bioelectrochemistry* 133:107447.
- Liu CC, Liu CC, Kanekiyo T, Xu H, Bu G (2013) Apolipoprotein E and Alzheimer disease: risk, mechanisms and therapy. *Nat Rev Neurol* 9:106–118.
- Liu CY, Ohki Y, Tomita T, Osawa S, Reed BR, Jagust W, Van Berlo V, Jin L-W, Chui HC, Coppola G, Ringman JM (2017) Two novel mutations in the first transmembrane domain of presenilin1 cause young-onset Alzheimer's disease. *J Alzheimers Dis* 58:1035–1041.
- Mahley RW (1988) Apolipoprotein E: cholesterol transport protein with expanding role in cell biology. *Science* 240:622–630.

- Michikawa M, Fan QW, Isobe I, Yanagisawa K (2000) Apolipoprotein E exhibits isoform-specific promotion of lipid efflux from astrocytes and neurons in culture. *J Neurochem* 74:1008–1016.
- Parcon PA, Balasubramaniam M, Ayyadevara S, Jones RA, Liu L, Shmookler Reis RJ, Barger SW, Mrak RE, Griffin WST (2018) Apolipoprotein E4 inhibits autophagy gene products through direct, specific binding to CLEAR motifs. *Alzheimers Dement* 14:230–242.
- Scheltens P, Blennow K, Breteler MM, de Strooper B, Frisoni GB, Salloway S, Van der Flier WM (2016) Alzheimer's disease. *Lancet* 388:505–517.
- Scheuner D, Eckman C, Jensen M, Song X, Citron M, Suzuki N, Bird TD, Hardy J, Hutton M, Kukull W, Larson E, Levy-Lahad L, Viitanen M, Peskind E, Poorkaj P, Schellenberg G, Tanzi R, Wasco W, Lannfelt L, Selkoe D, Younkin S (1996) Secreted amyloid β -protein similar to that in the senile plaques of Alzheimer's disease is increased in vivo by the presenilin 1 and 2 and APP mutations linked to familial Alzheimer's disease. *Nat Med* 2:864–870.
- Sogorb-Esteve A, García-Ayllón MS, Llansola M, Felipo V, Blennow K, Sáez-Valero J (2018) Inhibition of γ -secretase leads to an increase in presenilin-1. *Mol Neurobiol* 55:5047–5058.
- Steiner H, Romig H, Grim MG, Philipp U, Pesold B, Citron M, Baumeister R, Haass C (1999) The biological and pathological function of the presenilin-1 Δ Exon 9 mutation is independent of its defect to undergo proteolytic processing. *J Biol Chem* 274:7615–7618.
- Steiner H, Winkler E, Edbauer D, Prokop S, Basset G, Yamasaki A, Kostka M, Haass C (2002) PEN-2 is an integral component of the γ -secretase complex required for coordinated expression of presenilin and nicastrin. *J Biol Chem* 277:39062–39065.
- Strittmatter WJ, Saunders AM, Schmechel D, Pericak-Vance M, Enghild J, Salvesen GS, Roses AD (1993) Apolipoprotein E: high-avidity binding to beta-amyloid and increased frequency of type 4 allele in late-onset familial Alzheimer disease. *Proc Natl Acad Sci U S A* 90:1977–1981.
- Sun L, Zhou R, Yang G, Shi Y (2017) Analysis of 138 pathogenic mutations in presenilin-1 on the in vitro production of A β 42 and A β 40 peptides by γ -secretase. *Proc Natl Acad Sci U S A* 114:E476–E485.
- Takasugi N, Tomita T, Hayashi I, Tsuruoka M, Niimura M, Takahashi Y, Thinakaran G, Iwatsubo T (2003) The role of presenilin cofactors in the γ -secretase complex. *Nature* 422:438–441.
- Theendakara V, Peters-Libeu CA, Spilman P, Poksay KS, Bredesen DE, Rao RV (2016) Direct transcriptional effects of apolipoprotein E. *J Neurosci* 36:685–700.
- Watanabe H, Shen J (2017) Dominant negative mechanism of presenilin-1 mutations in FAD. *Proc Natl Acad Sci U S A* 114:12635–12637.
- Watanabe N, Tomita T, Sato C, Kitamura T, Morohashi Y, Iwatsubo T (2005) Pen-2 is incorporated into the γ -secretase complex through binding to transmembrane domain 4 of presenilin 1. *J Biol Chem* 280:41967–41975.
- Wernette-Hammond ME, Lauer SJ, Corsini A, Walker D, Taylor JM, Rall SC Jr (1989) Glycosylation of human apolipoprotein E. The carbohydrate attachment site is threonine. *J Biol Chem* 264:9094–9101.
- Yamazaki Y, Zhao N, Caulfield TR, Liu CC, Bu G (2019) Apolipoprotein E and Alzheimer disease: pathobiology and targeting strategies. *Nat Rev Neurol* 15:501–518.
- Yasuda M, Maeda K, Hashimoto M, Yamashita H, Ikejiri Y, Bird TD, Tanaka C, Schellenberg GD (1999) A pedigree with a novel presenilin 1 mutation at a residue that is not conserved in presenilin 2. *Arch Neurol* 56:65–69.
- Zhang S, Zhang M, Cai F, Song W (2013) Biological function of presenilin and its role in AD pathogenesis. *Transl Neurodegener* 2:15.
- Zhang Y-w, Luo W-j, Wang H, Lin P, Vetrivel KS, Liao F, Li F, Wong PC, Farquhar MG, Thinakaran G, Xu H (2005) Nicastrin is critical for stability and trafficking but not association of other presenilin/ γ -secretase components. *J Biol Chem* 280:17020–17026.
- Zhao G, Liu Z, Ilagan MX, Kopan R (2010) γ -secretase composed of PS1/Pen2/Aph1a can cleave notch and amyloid precursor protein in the absence of nicastrin. *J Neurosci* 30:1648–1656.
- Zou K, Yamaguchi H, Akatsu H, Sakamoto T, Ko M, Mizoguchi K, Gong J-S, Yu W, Yamamoto T, Kosaka K, Yanagisawa K, Michikawa M (2007) Angiotensin-converting enzyme converts amyloid β -protein 1-42 (A β (1-42)) to A β (1-40), and its inhibition enhances brain A β deposition. *J Neurosci* 27:8628–8635.
- Zou K, Hosono T, Nakamura T, Shiraiishi H, Maeda T, Komano H, Yanagisawa K, Michikawa M (2008) Novel role of presenilins in maturation and transport of integrin β 1. *Biochemistry* 47:3370–3378.